



## SYNTHESIS OF MESOPOROUS NANOPARTICLES VIA MICROWAVE-ASSISTED METHOD FOR PHOTOCATALYTIC DEGRADATION OF PHENOL DERIVATIVES

(Sintesis Nanopartikel Bermesoliang Melalui Kaedah Bantuan-Gelombang Mikro untuk Degradasi Fotomangkin daripada Terbitan Fenol)

Nur Farhana Jaafar<sup>1\*</sup>, Nor Amira Marfur<sup>1</sup>, Nurfatehah Wahyuni Che Jusoh<sup>2</sup>, Yuki Nagao<sup>3</sup>, Nur Hidayatul Nazirah Kamarudin<sup>4,5</sup>, Rohayu Jusoh<sup>6</sup>, Mohammad Anwar Mohamed Iqbal<sup>1</sup>

<sup>1</sup>School of Chemical Sciences,

Universiti Sains Malaysia, 11800 USM Penang, Malaysia

<sup>2</sup>Department of Chemical Process Engineering, Malaysia-Japan International Institute of Technology (MJIT),  
Universiti Teknologi Malaysia Kuala Lumpur, Jalan Sultan Yahya Petra, 54100 Kuala Lumpur, Malaysia

<sup>3</sup>School of Materials Science,

Japan Advanced Institute of Science and Technology, 1-1 Asahidai, Nomi, Ishikawa 923-1292, Japan

<sup>4</sup>Research Center for Sustainable Process Technology (CESPRO),

<sup>5</sup>Chemical Engineering Programme, Faculty of Engineering and Built Environment,

Universiti Kebangsaan Malaysia, 43600 UKM Bangi, Selangor, Malaysia

<sup>6</sup>Faculty of Chemical and Natural Resources Engineering,

Universiti Malaysia Pahang, Lebuhraya Tun Razak, 26300 Gambang, Kuantan, Pahang, Malaysia

\*Corresponding author: [nurfarhana@usm.my](mailto:nurfarhana@usm.my)

Received: 14 January 2019; Accepted: 26 April 2019

### Abstract

Mesoporous transition metal oxides have gained attention widely since they possess both optical and electronic properties of transition metal oxides especially for photocatalytic degradation application. In this research work, mesoporous titania nanoparticles (MTN) and mesoporous zinc oxide nanoparticles (MZN) were successfully synthesized using microwave (MW)-assisted method to degrade phenol derivatives under visible light irradiation. The microwave sintering effect on the surface of these modified structures was studied to relate with their photocatalytic performance. The characterization results indicated that MW-assisted method was mainly contributed in generating  $Ti^{3+}$  site defects (TSD) and oxygen vacancies (OV) in MTN while for MZN contained only OV as one of the strategies in light-absorption modification for  $TiO_2$  and ZnO to enhance their photoactivity. MTN also showed the degradation of 2-chlorophenol was up to 97% while degradation of phenol by MZN was up to 87%.

**Keywords:** mesoporous nanoparticles, titanium dioxide, zinc oxide, microwave-assisted, photocatalytic

### Abstrak

Logam oksida peralihan bermesoliang telah mendapat perhatian secara meluas kerana mereka mempunyai kedua-dua sifat optik dan elektronik bagi oksida logam peralihan terutamanya untuk aplikasi degradasi fotomangkin. Dalam kajian ini, nanopartikel titania bermesoliang (MTN) dan nanopartikel zink oksida bermesoliang (MZN) telah berjaya disintesis menggunakan kaedah bantuan-gelombang mikro (MW) untuk mendegradasi terbitan fenol di bawah sinaran cahaya nampak. Kesan pensinteran gelombang mikro pada permukaan struktur yang diubahsuai telah dikaji untuk dikaitkan dengan prestasi fotomangkin mereka. Keputusan pencirian menunjukkan bahawa kaedah bantuan-MW merupakan penyumbang utama dalam pembentukan tapak  $Ti^{3+}$  cacat (TSD) dan kekosongan oksigen permukaan (OV) dalam MTN manakala bagi MZN hanya mengandungi OV sebagai salah

satu strategi untuk pengubahsuaian penyerapan-cahaya bagi TiO<sub>2</sub> and ZnO untuk meningkatkan fotoaktiviti mereka. MTN juga menunjukkan degradasi 2-klorofenol sehingga 97% manakala degradasi fenol oleh MZN sehingga 87%.

**Kata kunci:** nanopartikel bermesolintang, titanium dioksida, zink oksida, bantuan-gelombang mikro, fotomangkin

### Introduction

Among various semiconductors, TiO<sub>2</sub> and ZnO are the most promising photocatalysts since they possess good photosensitivity and chemical stability besides non-toxic and low cost. TiO<sub>2</sub> is generally used in production of sunscreen, dye sensitized solar cells, orthopedic and pharmaceutical field [1-3]. On the other hand, ZnO is frequently used in the production of biodiesel, supercapacitor, water purification and biomedical industries [4-7]. However, they are affected by some limitations related to optical and electronic properties [8, 9]. TiO<sub>2</sub> and ZnO have a large band gap which is 3.20 eV and 3.37 eV, respectively [10, 11]. Their wide band gap can reduce their photocatalytic performance in the UV wavelength region which contributes around 3 to 5% of the total solar spectrum. Hence, these photocatalysts are highly active under UV light illumination rather than visible light irradiation. Besides that, fast recombination of photo-induced holes and electrons may restrict their photodegradation efficiency. Therefore, major energy loss and very low photocatalytic reaction occur resulting from significant absence of electron donors or acceptors [12, 13].

Nowadays, mesoporous transition metal oxides have been studied widely since they are well known for having both optical and electronic properties of transition metal oxides. These properties give many advantages for different applications since it can have various morphologies and compositions including fibers, nanoparticles, monoliths and thin films besides possess large and uniform pore size which increase high surface area and long range of ordering structure also tunable pore diameter [14].

Through (MW)-assisted process, the efficiency of these photocatalysts can be enhanced since this method to increase their porosity and generate numerous site defects which are TSD and OV for MTN and OV for MZN [15-19]. Microwave is an essential appliance practically in most kitchens. This appliance is beneficial in term of time's consumption and energy savings compared to traditional food preparation methods [20]. Different methods have been investigated to synthesize mesoporous nanoparticles including e-beam irradiation, high-temperature hydrogenation, plasma treatment, sol-gel and vacuum activation [21-24]. However, these synthesis methods involve uneven temperature distribution, long reaction time and reduction conditions. (MW)-assisted process has been successfully demonstrated as being fast and effective in the preparation of mesoporous materials [25-27].

Generally, the microwave radiation will heat the reactants but not the reaction container itself as the radiation passes through the walls of the container. Process of microwave heating involve the transferring of electromagnetic energy to thermal energy. Heat also can be supplied throughout the sample since microwaves capable in penetrating the materials and storing energy [28]. Particularly, energy transfer has the potential to reach a uniform and heat the thick materials in the short time since it does not depend on the heat dispersion from the surfaces. Hence, the heating can be uniform throughout the material and may lead to less formation of by-products and/or decomposition products, if the machine is well-designed. In addition, the microwave energy is capable to increase the heating rate, decrease the kinetics of crystallization and potentially form new metastable phases [29]. This method also provides a uniform and speedy reaction environment to produce materials with homogenous and dispersed morphology [30]. Nevertheless, the popularity of using (MW)-assisted process in synthesizing mesoporous nanomaterial keep increasing due to its various benefits such as shorter the reaction times, heating of selective material, transferring of energy instead of heat, volumetric heating ability, obtaining high purity materials and heating starts from interior of material body and in many cases smaller particle sizes [31].

Use of MTN and MZN as photocatalyst usually applies in Advanced oxidation process (AOP). AOP is a set of chemical treatment methods to degrade the organic and inorganic material in wastewater thru oxidation. Photocatalytic degradation is one of AOPs procedures that promote the generation of electron-hole pairs once the photon excited from the valance band (VB) to the conduction band (CB) when the catalyst irradiated by light. Besides that, this process has demonstrated a great potential for wastewater treatment method to degrade organic pollutant and mainly suitable for the removal of non-biodegradable materials such as aromatics, petroleum

constituent, pesticides and volatile organic in wastewater. Through this process, the pollutant materials are converted into stable inorganic compounds such as carbon dioxide and water which are less hazardous [32-35].

Chlorophenol is a common pollutant released from industrial parks into aqueous environmental system which has gained a great concern due to their high toxicity, stability and potentially carcinogenic. Therefore, there are many studies conducted regarding the appropriate methods to eliminate these compounds to decrease the adverse effect toward the environment and humans. Based on the Environmental Quality Act 1979 (Sewage and Industrial Effluent), Department of Environment (DOE) in Malaysia has gazette allowable limit that this pollutant should be treated not more than  $1 \text{ mg L}^{-1}$  before being released to the environment as they can affect the odor and taste of drinking water with concentrations as low as a few  $\mu\text{g L}^{-1}$ .

In this study, (MW)-assisted process was used to synthesized MTN and MZN to degrade 2-chlorophenol and phenol, respectively under visible light irradiation. The effect of microwave sintering on the surface of these modified structures regarding to generation of site defects which were TSD and OV in MTN while for MZN contained only OV were studied as one of the strategies in light-absorption modification for  $\text{TiO}_2$  and ZnO to enhance their photocatalytic performance.

## **Materials and Methods**

### **Reagents and material**

Titanium (IV) isopropoxide (TTIP), zinc acetate and sodium dodecyl sulfate (SDS) surfactant were bought from Sigma-Aldrich. 2-propanol, phenol and hydrochloric acid (HCl) were purchased from MERCK, Malaysia. Acetone and methanol were purchased from RPE Reagent pure Erba. Sodium hydroxide (NaOH) and ammonium hydroxide ( $\text{NH}_4\text{OH}$ ) were purchased from QREC<sup>TM</sup> and 2-chlorophenol (2-CP) from Alfa Aesar, Germany with 99% purity.

### **Synthesis of mesoporous nanoparticles**

The mesoporous titania nanoparticles (MTN) was synthesized by the microwave (MW)-assisted process. SDS surfactant was dissolved in distilled water, 2-propanol and ammonia solution. The mixture was stirred continuously for 30 minutes at  $50 \text{ }^\circ\text{C}$  in water bath. Then, titanium (IV) isopropoxide (TTIP) was added into the mixture and continued stirring for 2 hours at  $80 \text{ }^\circ\text{C}$  before placing in the MW. MW heating was conducted in a domestic MW oven (Samsung ME711K), which can be operated with power ranging from 100-800 W and frequency of 2.45 GHz. The power density of MW was adjusted with  $0.56 \text{ Wg}^{-1}$  and the heating of the mixture was continued for 2 hours to allow the formation of sol-gel. The obtained product was collected and dried overnight in an oven before calcined at  $600 \text{ }^\circ\text{C}$  for 3 hours. This procedure was applied in the synthesis of mesoporous zinc oxide nanoparticles (MZN) except the TTIP was replaced with zinc acetate and the obtained product was calcined at  $550 \text{ }^\circ\text{C}$  for 3 hours.

### **Material characterization**

The chemical oxidation of the catalysts was determined using X-ray photoelectron spectroscopy (XPS) conducted on a Kratos Ultra spectrometer equipped with an Mg  $K\alpha$  radiation source (10 mA, 15 kV). The crystalline structures of the catalysts were carried out using a Bruker Advance D8 X-ray powder diffractometer (XRD). The band gap of the catalysts was measured using UV-Vis diffuse reflectance spectra (UV-Vis DRS) using Perkin-Elmer Lambda 900 UV/VIS/NIR spectrometer with an integrating sphere. Nitrogen adsorption-desorption isotherms were used to determine the textural properties at liquid nitrogen temperatures using a SA 3100 Surface Analyzer (Beckman Coulter). The Brunauer-Emmett-Teller (BET) was used to calculate surface area of the catalyst.

### **Photodegradation of phenol derivatives**

The photoactivity of the MTN and MZN was tested on degradation of 2-CP and phenol, respectively. The photocatalytic experiments were performed in a batch reactor with connected to 48 W fluorescence lamp as a visible light source. For photoactivity process, 0.075 g of catalyst was added to the solution with the desired concentration (200 mL) and stirred for 1 h in the dark condition to achieve adsorption-desorption equilibrium before continued for another 6 h under light irradiation. During the reaction, aliquots of 2 mL were taken out at intervals of 30 min and centrifuged in a Hettich Zentrifugen Micro 120 at 15000 rpm for 15 minutes before being analyzed by UV-Vis spectrophotometry (Shimadzu UV-Vis Spectrometer, UV-2600) for determination of residual concentration of

solution. Each set of experiments was performed triplicates. The adsorption band of 2-CP and phenol was taken at 274 and 270 nm, respectively. The percentage degradation was calculated using the following equation 1:

$$\text{Degradation (\%)} = \frac{c_i - c_t}{c_i} \times 100 \quad (1)$$

where  $C_i$  and  $C_t$  are the initial concentration 2-CP and the concentration at time  $t$ , respectively.

## Results and Discussion

### Characterization of the catalysts

Fig. 1 shows the XRD diffractogram of MTN (Figure 1a) and MZN (Figure 1b). Figure 1a demonstrated a series of XRD peaks for the  $\text{TiO}_2$  anatase phase was observed at  $25.3^\circ$  (101),  $37^\circ$  (004),  $38^\circ$  (112),  $48^\circ$  (200),  $53^\circ$  (105) and  $55^\circ$  (211). Other than anatase phase,  $\text{TiO}_2$  rutile phase was detected at  $28^\circ$  (110) and  $54^\circ$  (211) as well as brookite phase at  $32^\circ$  (121). The MZN (Figure 1b) demonstrated all the peaks are fits with the hexagonal wurtzite structure of ZnO (JCPDS No. 01-072-2743). A series of XRD peaks for the ZnO at  $31^\circ$ ,  $34.4^\circ$ ,  $36^\circ$ ,  $47.3^\circ$ ,  $57^\circ$ ,  $63^\circ$ ,  $67.9^\circ$  and  $69.5^\circ$  were corresponding to (100), (002), (101), (102), (110), (103), (112) and (201) planes, respectively. It can be observed that both catalysts illustrated a good crystallinity, degree of orderliness and mesoporous uniformity where indicated that MW-assisted method efficaciously provide a good heat distribution during synthesis by heating the entire reaction solution with proper temperature to improve the structural arrangement [36].

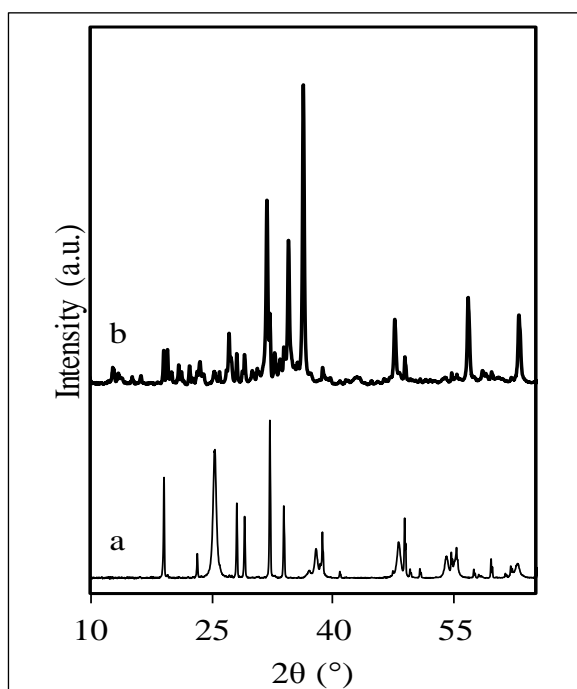


Figure 1. XRD diffractograms of (a) MTN and (b) MZN

The chemical states of MTN and MZN were determined using XPS as showed in Figure 2. Figure 2a shows the  $\text{Ti}2p$  spectrum of MTN in the region of 454-470 eV. The  $\text{Ti}2p$  can be fixed into five peaks which are at 458.2 ( $\text{Ti}2p_{3/2}$ ), 459 ( $\text{Ti}2p_{3/2}$ ) and 462.5 ( $\text{Ti}2p_{1/2}$ ) eV were assigned to  $\text{Ti}^{3+}$ , while the peaks at 455.6 ( $\text{Ti}2p_{3/2}$ ) and 465.2 ( $\text{Ti}2p_{1/2}$ ) eV were attributed to  $\text{Ti}^{4+}$  [37]. The  $\text{O}1s$  spectrum of MTN (Figure 2b) illustrated the presence of  $\text{Ti}^{4+}\text{-O}$  peaks at 529.8 and 533.5 eV, whereas peaks at 530.2 and 532.6 eV is attributed to  $\text{Ti}^{3+}\text{-O}$  and hydroxide or hydroxyl group ( $\text{OH}^-$ ), respectively [38]. According to Naeem et al. the development of  $\text{OH}^-$  peak indicated the presence of OV in the catalyst [39]. The oxidation state of Zn in MZN (Figure 2c) was illustrated by Zn2p doublet peaks at 1018

eV ( $Zn2p_{3/2}$ ) and 1041 eV ( $Zn2p_{1/2}$ ) indicated the oxidation state of Zn is  $2+$  where the different in binding energy for both peaks are 23 eV which further confirmed the characteristic of a  $Zn^{2+}$  oxidation state in ZnO wurtzite structure [40]. Figure 2d shows the O1s spectrum of MZN can be fixed into three peaks at 528.35, 530 and 533 eV. The peak at 528.35 eV was attributed to  $O^{2-}$  ions in ZnO wurtzite structure of hexagonal  $Zn^{2+}$  which can be illustrated as Zn-O bonds [41]. The presence of OV in the MZN can be detected at peak 530 eV where this peak illustrated the  $O^{2-}$  in the oxygen deficient regions with the matrix of ZnO [42], while the highest peak at 533 eV was assigned to the presence of loosely bound oxygen on the surface of ZnO [43]. These results confirmed the presence of TSD and OV in the MTN as well as OV in MZN where it is a good prospective because the photocatalyst depends mainly on the OV and TSD especially for application under visible light irradiation.

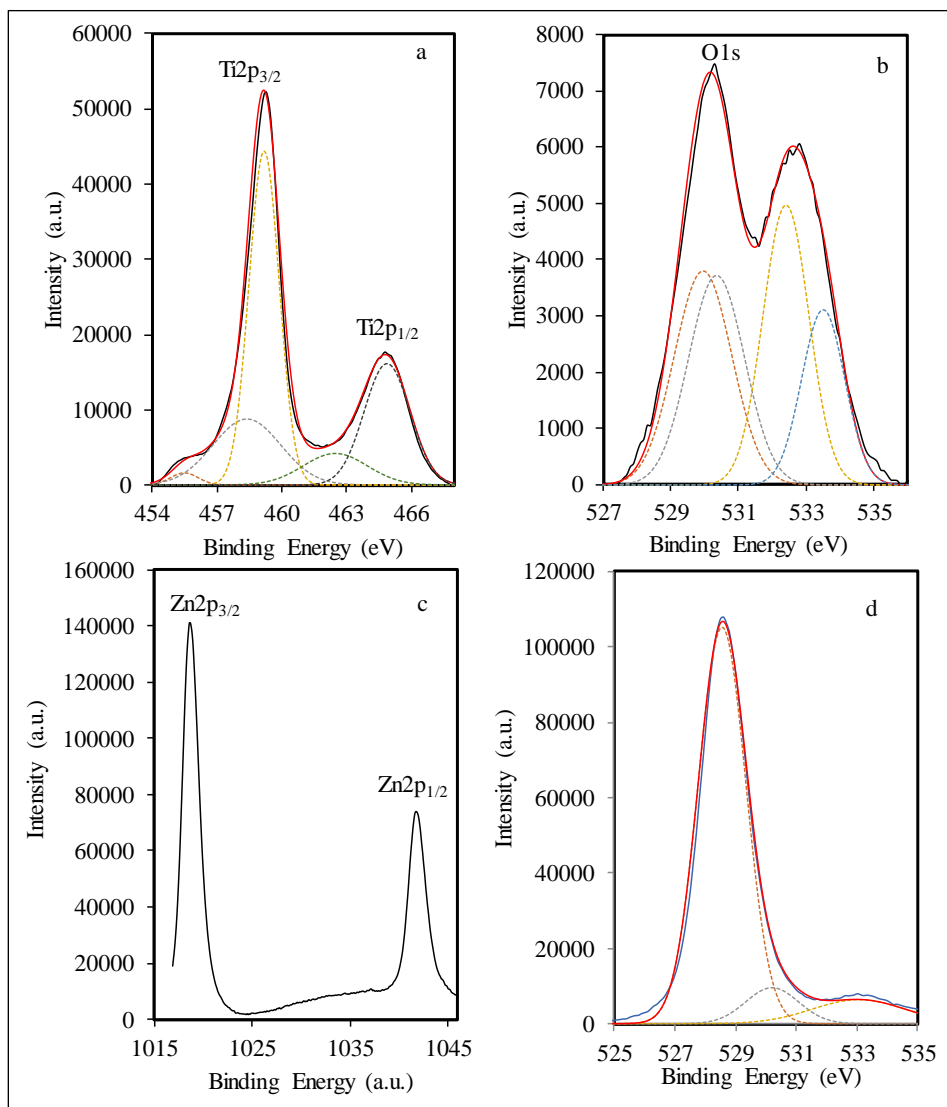


Figure 2. XPS spectra of (a) Ti2p and (b) O1s of MTN, (c) Zn2p and (d) O1s of MZN

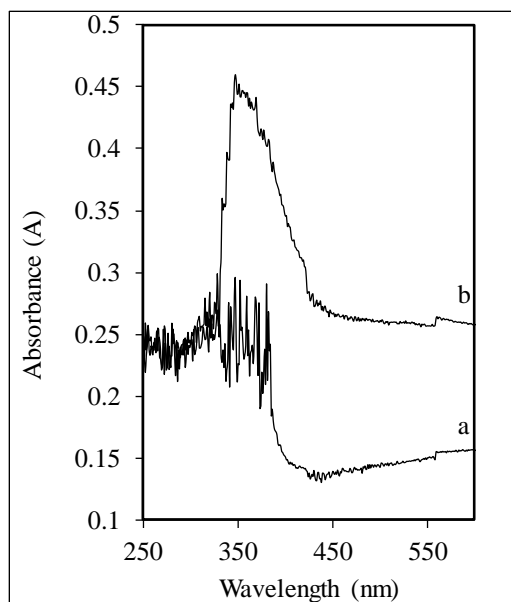


Figure 3. UV-Vis diffuse reflectance spectra at range 250-600 nm of (a) MTN and (b) MZN

Based on the characterization results, it's revealed that MW-assisted method was successfully synthesized MTN and MZN. This method shows potential for self-modified MTN containing TSD and OV, while and MZN containing OV as one of the strategies in light-absorption modification for  $\text{TiO}_2$  and  $\text{ZnO}$  to enhance their photoactivity. This method promising limit time required in synthesis of catalyst compared with other conventional chemical synthesis method where it's allowed the hydrolysis and condensation processes occurred during the microwave electromagnetic radiation (red arrow) after the precursor formed at the template created by SDS. In addition, it also demonstrated as being effective in the preparation of mesoporous materials since can provide a uniform and fast reaction environment to produce materials with homogenous and dispersed morphology [40]. The microwave energy is capable to increase the heating rate, reduce the kinetics of crystallization and potentially form new metastable phases [29]. This method affects the nucleation without having direct contact between the reacting chemicals and energy sources which demonstrates that the volumetric heating is not involving the heat diffusion or the wall [26]. Furthermore, the microwave energy is directly applied to the solution over molecular interaction with the electromagnetic field. The heat generated in this method pass throughout the material uniformly resulting good in the sintering by inhibits the particle growth. Figure 4 shows the schematic diagram of MW-assisted process. The particle growth may also reduce during the heat treatment which leading to a higher surface area and improve the catalyst efficiency. Electromagnetic wave in microwave caused the water dipole rotation and ion oscillation on crystallization mechanism which may differ from conventional heating.

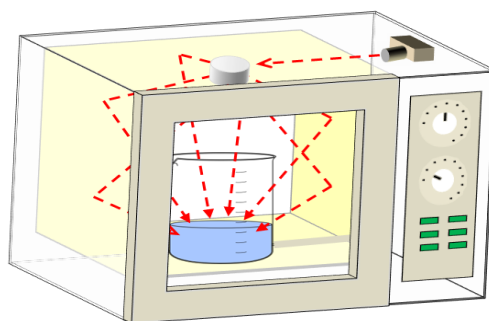


Figure 4. Schematic diagram of microwave-assisted process

### Catalytic testing on photodegradation of phenol derivatives

The photocatalytic activity of MTN and MZN was tested on the degradation of phenol derivatives under visible light irradiation as showed in Figure 5. It was after 6h irradiation clearly observed that both catalysts successfully degrade 97% and 88% of 2-CP (MTN) and phenol (MZN), respectively. The 2-CP was almost successfull degraded by MTN probably due to the presence of TSD and OV which may acted as electron acceptors to lesson electron hole recombination and improves the photoactivity although the band gap in the UV range. Generally, the MTN required energy larger or equal than 387.5 nm to excite the electron from the valance band (VB) to the conduction band (CB). However, the presence of TSD and OV allowed the electrons to excite from VB to TSD and OV as well as from TSD and OV to CB [19]. Their presence not only facilitates the electrons excitation but also allowed the photoactivity undergoes under visible light irradiation since the electrons can be excited from VB, TSD and OV. In contrast, the band gap of MZN has been allowed to be applied under visible light but the presence of OV in MZN may inhibit the electron-hole recombination to enhance the photoactivity. The stability and reusability of the catalysts were further studied by repeating a series of experiments in degrading 2-CP and phenol for MTN and MZN, respectively as demonstrated in Figure 6. In each new cycle, the catalyst was collected, washed and calcined according to synthesis procedure before being used for degradation of a fresh 2-CP or phenol solution. Figure 6 illustrated that both catalysts were still active with the slight decrease after five repetition of experiment. The MTN shows the degradation of 2-CP was decreased from 97% to 86%, while degradation of phenol by MZN decrease from 87% to 79%. These results reveal that both catalysts have a good stability and potentially to use repeatly under visible light irradiation.

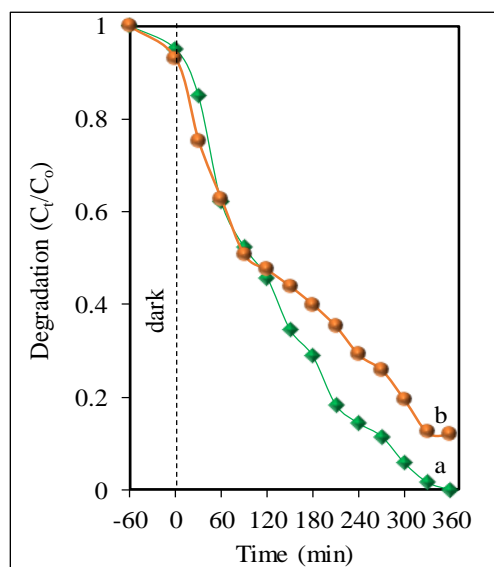


Figure 5. Photocatalytic performance of (a) MTN and (b) MZN for degradation of 2-CP and phenol, respectively [C<sub>2-CP/phenol</sub>: 10 ppm, pH: 5, W<sub>catalyst</sub>: 0.075 g, t: 360 min]

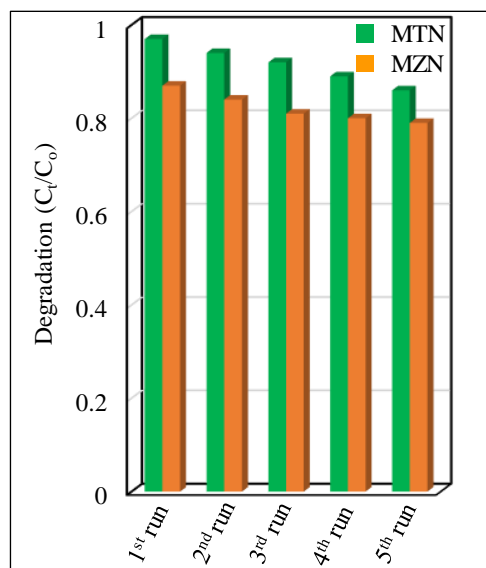


Figure 6. Regeneration study of MTN and MZN for degradation of 2-CP and phenol, respectively [ $C_{2-CP/phenol}$ : 10 ppm, pH: 5,  $W_{catalyst}$ : 0.075 g, t: 360 min]

### Conclusion

We successfully synthesized MTN and MZN *via* MW-assisted process using different precursors to degrade different chlorophenols under visible light radiation. Based on the XPS results, the microwave sintering effect on the surface of these modified structures has generated TSD and OV in MTN while MZN contained only OV which have significantly enhanced their photocatalytic performance. XRD results indicated that both catalysts demonstrated a good crystallinity, degree of orderliness and mesoporous uniformity where indicated that MW-assisted method efficaciously provides a good heat distribution during synthesis by heating the entire reaction solution with proper temperature to improve the structural arrangement. Therefore, this method has high potential to be used in synthesizing mesoporous materials due to its sintering effects. MTN also had degraded about 97% of 2-CP while MZN had degraded around 87% of phenol.

### Acknowledgement

The authors are grateful for the financial support by Ministry of Education Malaysia for Fundamental Research Grant Scheme (203.PKIMIA.6711607) and Universiti Sains Malaysia (USM) for Short Term Grant (304/PKIMIA/6315055).

### References

1. Aba-Guevara, C. G., Medina-Ramírez, I. E., Hernández-Ramírez, A., Jáuregui-Rincón, J., Lozano-Álvarez, J. A. and Rodríguez-López, J. L. (2017). Comparison of two synthesis methods on the preparation of Fe, N-Co-doped TiO<sub>2</sub> materials for degradation of pharmaceutical compounds under visible light. *Ceramics International*, 43(6): 5068-5079.
2. Reinoso, J. J., Docio, C. M. Á., Ramírez, V. Z. and Lozano, J. F. F. (2018). Hierarchical nano ZnO-micro TiO<sub>2</sub> composites: High UV protection yield lowering photodegradation in sunscreens. *Ceramics International*, 44(3): 2827-2834.
3. Zhu, M., Chen, L., Gong, H., Zi, M. and Cao, B. (2014). A novel TiO<sub>2</sub> nanorod/nanoparticle composite architecture to improve the performance of dye-sensitized solar cells. *Ceramics International*, 40(1): 2337-2342.
4. Baskar, G. and Soumiya, S. (2016). Production of biodiesel from castor oil using iron(II) doped zinc oxide nanocatalyst. *Renewable Energy*, 98: 101-107.



5. Khatami, M., Alijani, H. Q., Heli, H. and Sharifi, I. (2018). Rectangular shaped zinc oxide nanoparticles: Green synthesis by Stevia and its biomedical efficiency. *Ceramics International*, 44: 15596-15602.
6. Prasankumar, T., Aazem, V.I., Raghavan, P., Ananth, K.P., Biradar, S., Ilangovan, R. and Jose, S. (2017). Microwave assisted synthesis of 3D network of Mn/Zn bimetallic oxide-high performance electrodes for supercapacitors. *Journal of Alloys and Compounds*, 695: 2835-2843.
7. Mirzaei, A., Yerushalmi, L., Chen, Z., Haghghat, F. and Guo, J. (2018). Enhanced photocatalytic degradation of sulfamethoxazole by zinc oxide photocatalyst in the presence of fluoride ions: Optimization of parameters and toxicological evaluation. *Water Research*, 132: 241-251.
8. Li, F. B. and Li, X. Z. (2002). The enhancement of photodegradation efficiency using Pt-TiO<sub>2</sub> catalyst. *Chemosphere*, 48(10): 1103-1111.
9. Houshmand, A., Daud, W. M. A. W. and Shafeeyan, M. S. (2011). Tailoring the surface chemistry of activated carbon by nitric acid: study using response surface method. *Bulletin of the Chemical Society of Japan*, 84(11): 1251-1260.
10. Khan, M. M., Lee, J. and Cho, M. H. (2014). Au@TiO<sub>2</sub> nanocomposites for the catalytic degradation of methyl orange and methylene blue: An electron relay effect. *Journal of Industrial and Engineering Chemistry*, 20(4): 1584-1590.
11. Ahmad, M., Ahmed, E., Hong, Z. L., Jiao, X. L., Abbas, T. and Khalid, N. R. (2013). Enhancement in visible light-responsive photocatalytic activity by embedding Cu-doped ZnO nanoparticles on multi-walled carbon nanotubes. *Applied Surface Science*, 285: 702-712.
12. Pouran, S. R., Bayrami, A., Aziz, A. A., Daud, W. M. A. W. and Shafeeyan, M. S. (2016). Ultrasound and UV assisted Fenton treatment of recalcitrant wastewaters using transition metal-substituted-magnetite nanoparticles. *Journal of Molecular Liquids*, 222: 1076-1084.
13. Zheng, X., Li, D., Li, X., Chen, J., Cao, C., Fang, J., Wang, J., He, Y. and Zheng, Y. (2015). Construction of ZnO/TiO<sub>2</sub> photonic crystal heterostructures for enhanced photocatalytic properties. *Applied Catalysis B: Environmental*, 168: 408-415.
14. Faisal, M., Bouzid, H., Harraz, F. A., Ismail, A. A., Al-Sayari, S. A. and Al-Assiri, M. S. (2015). Mesoporous Ag/ZnO multilayer films prepared by repeated spin-coating for enhancing its photonic efficiencies. *Surface and Coatings Technology*, 263: 44-53.
15. Anas, S., Rahul, S., Babitha, K. B., Mangalaraja, R. V. and Ananthakumar, S. (2015). Microwave accelerated synthesis of zinc oxide nanoplates and their enhanced photocatalytic activity under UV and solar illuminations. *Applied Surface Science*, 355: 98-103.
16. Jaafar, N. F. and Jalil, A. A. (2018). Photocatalytic degradation of phenol derivatives over silver supported on mesoporous titania nanoparticles. *Malaysian Journal of Analytical Sciences*, 22(5): 807-816.
17. Kajbafvala, A., Zanganeh, S., Kajbafvala, E., Zargar, H. R., Bayati, M. R. and Sadrnezhaad, S. K. (2010). Microwave-assisted synthesis of narciss-like zinc oxide nanostructures. *Journal of Alloys and Compounds*, 497 (1-2): 325-329.
18. Tripathy, N., Ahmad, R., Kuk, H., Hahn, Y. B. and Khang, G. (2016). Mesoporous ZnO nanoclusters as an ultra-active photocatalyst. *Ceramics International*, 42(8): 9519-9526.
19. Jaafar, N. F., Jalil, A. A., Triwahyono, S. and Shamsuddin, N. (2015). New insights into self-modification of mesoporous titania nanoparticles for enhanced photoactivity: Effect of microwave power density on formation of oxygen vacancies and Ti<sup>3+</sup> defects. *RSC Advances*, 5(110): 90991-91000.
20. Thostenson, E. T. and Chou, T. W. (1999). Microwave processing: fundamentals and applications. *Composites Part A: Applied Science and Manufacturing*, 30(9): 1055-1071.
21. Hoang, S., Berglund, S. P., Hahn, N. T., Bard, A. J. and Mullins, C. B. (2012). Enhancing visible light photo-oxidation of water with TiO<sub>2</sub> nanowire arrays via cotreatment with H<sub>2</sub> and NH<sub>3</sub>: Synergistic effects between Ti<sup>3+</sup> and N. *Journal of the American Chemical Society*, 134(8): 3659-3662.
22. Zhang, Z. K., Bai, M. L., Guo, D. Z., Hou, S. M. and Zhang, G. M. (2011). Plasma-electrolysis synthesis of TiO<sub>2</sub> nano/microspheres with optical absorption extended into the infra-red region. *Chemical Communications*, 47(29): 8439-8441.
23. Yuan, Z., Xiao-Xuan, W., Lv, H. and Wen-Chen, Z. (2007). EPR parameters and defect structures of the off-center Ti<sup>3+</sup> ion on the Sr<sup>2+</sup> site in neutron-irradiated SrTiO<sub>3</sub> crystal. *Journal of Physics and Chemistry of Solids*, 68(9): 1652-1655.

24. Bromiley, G. D. and Shiryaev, A. A. (2006). Neutron irradiation and post-irradiation annealing of rutile ( $\text{TiO}_{2-x}$ ): effect on hydrogen incorporation and optical absorption. *Physics and Chemistry of Minerals*, 33(6): 426-434.
25. Suwarnkar, M. B., Dhabbe, R. S., Kadam, A. N. and Garadkar, K. M. (2014). Enhanced photocatalytic activity of Ag doped  $\text{TiO}_2$  nanoparticles synthesized by a microwave assisted method. *Ceramics International*, 40(4): 5489-5496.
26. Zhou, H., Tan, X., Huang, J. and Chen, X. (2017). Sintering behavior, phase evolution and microwave dielectric properties of thermally stable  $\text{Li}_2\text{O}-3\text{MgO}-m\text{TiO}_2$  ceramics ( $1 \leq m \leq 6$ ). *Ceramics International*, 43(4): 3688-3692.
27. Wang, W., Bai, W., Shen, B. and Zhai, J. (2015). Microwave dielectric properties of low temperature sintered  $\text{ZnWO}_4\text{-TiO}_2$  composite ceramics. *Ceramics International*, 41: S435-S440.
28. Kamarudin, N. H. N., Jalil, A. A., Triwahyono, S., Artika, V., Salleh, N. F. M., Karim, A. H., Jaafar, N. F., Sazegar, M. R., Mukti, R. R., Hameed, B. H. and Johari, A. (2014). Variation of the crystal growth of mesoporous silica nanoparticles and the evaluation to ibuprofen loading and release. *Journal of Colloid and Interface Science*, 421: 6-13.
29. Komarneni, S., Rajha, R. K. and Katsuki, H. (1999). Microwave-hydrothermal processing of titanium dioxide. *Materials Chemistry and Physics*, 61(1): 50-54.
30. Shi, M., Kang, L. and Jiang, Y. (2014). Microwave-assisted synthesis of mesoporous tungsten carbide/carbon for fuel cell applications. *Catalysis Letters*, 144(2): 278-284.
31. Clark, D. E., Folz, D. C. and West, J. K. (2000). Processing materials with microwave energy. *Materials Science and Engineering: A*, 287(2): 153-158.
32. Khaki, M. R. D., Shafeeyan, M. S., Raman, A. A. A. and Daud, W. M. A. W. (2017). Application of doped photocatalysts for organic pollutant degradation-A review. *Journal of Environmental Management*, 198: 78-94.
33. Antonopoulou, M., Evgenidou, E., Lambropoulou, D. and Konstantinou, I. (2014). A review on advanced oxidation processes for the removal of taste and odor compounds from aqueous media. *Water Research*, 53: 215-234.
34. Oturan, M. A. and Aaron, J. J. (2014). Advanced oxidation processes in water/wastewater treatment: principles and applications. A review. *Critical Reviews in Environmental Science and Technology*, 44(23): 2577-2641.
35. Bokare, A. D. and Choi, W. (2014). Review of iron-free Fenton-like systems for activating  $\text{H}_2\text{O}_2$  in advanced oxidation processes. *Journal of Hazardous Materials*, 275: 121-135.
36. Yuan, S., Sheng, Q., Zhang, J., Yamashita, H. and He, D. (2008). Synthesis of thermally stable mesoporous  $\text{TiO}_2$  and investigation of its photocatalytic activity. *Microporous and Mesoporous Materials*, 110(2-3): 501-507.
37. Khan, M. M., Ansari, S. A., Pradhan, D., Ansari, M. O., Lee, J. and Cho, M. H. (2014). Band gap engineered  $\text{TiO}_2$  nanoparticles for visible light induced photoelectrochemical and photocatalytic studies. *Journal of Materials Chemistry A*, 2(3): 637-644.
38. Huang, C.N., Bow, J.S., Zheng, Y., Chen, S.Y., Ho, N. and Shen, P. (2010). Nonstoichiometric titanium oxides via pulsed laser ablation in water. *Nanoscale research letters*, 5(6): 972-785.
39. Naeem, M., Hasanain, S. K., Kobayashi, M., Ishida, Y., Fujimori, A., Buzby, S. and Shah, S. I. (2006). Effect of reducing atmosphere on the magnetism of  $\text{Zn}_{1-x}\text{Co}_x\text{O}$  ( $0 \leq x \leq 0.10$ ) nanoparticles. *Nanotechnology*, 17(10): 2675-2680.
40. Bazant, P., Kuritka, I., Munster, L. and Kalina, L. (2015). Microwave solvothermal decoration of the cellulose surface by nanostructured hybrid Ag/ZnO particles: A joint XPS, XRD and SEM study. *Cellulose*, 22(2): 1275-1293.
41. Hsieh, P. T., Chen, Y. C., Kao, K. S. and Wang, C. M. (2008). Luminescence mechanism of ZnO thin film investigated by XPS measurement. *Applied Physics A*, 90(2): 317-321.
42. Katoch, A., Choi, S.W., Kim, H. W. and Kim, S. S. (2015). Highly sensitive and selective  $\text{H}_2$  sensing by ZnO nanofibers and the underlying sensing mechanism. *Journal of Hazardous Materials*, 286: 229-235.
43. Wang, J., Wang, Z., Huang, B., Ma, Y., Liu, Y., Qin, X., Zhang, X. and Dai, Y. (2012). Oxygen vacancy induced band-gap narrowing and enhanced visible light photocatalytic activity of ZnO. *ACS Applied Materials & Interfaces*, 4(8): 4024-4030.